



Magnetic anisotropy and orbital angular momentum in the orbital ferrimagnet CoMnO₃Hiroki Koizumi ¹, Jun-ichiro Inoue,¹ and Hideto Yanagihara ^{1,2}¹*Department of Applied Physics, University of Tsukuba, Tsukuba, Ibaraki 305-8573, Japan*²*Tsukuba Research Center for Energy Materials Science (TREMS), University of Tsukuba, Tsukuba, Ibaraki 305-8573, Japan*

(Received 19 October 2019; published 30 December 2019)

We investigated the temperature dependence of the saturation magnetization $M_S(T)$ and magnetic anisotropy constant $K_u(T)$ of CoMnO₃ with an ilmenite structure, which is known as an *orbital ferrimagnet*. Because of strong antiferromagnetic coupling between the Co²⁺ spin ($d^7: S = 3/2$) and Mn⁴⁺ spin ($d^3: S = 3/2$) in CoMnO₃, the net magnetic moment is considered to originate only from the orbital angular momentum [(OAM); $\langle L \rangle \approx 1$] of Co²⁺. Experimental results for CoMnO₃ epitaxial films clearly show that $K_u(T)$ is proportional to $M_S(T)$ for a wide temperature range up to the transition temperature, suggesting that $K_u(T)$ is proportional to $\langle L \rangle$. An electron theory based on the cluster model for K_u and the OAM of Co²⁺ at 0 K also indicates that K_u is proportional to the OAM and to the orbital angular anisotropy of Co²⁺.

DOI: [10.1103/PhysRevB.100.224425](https://doi.org/10.1103/PhysRevB.100.224425)**I. INTRODUCTION**

Magnetic anisotropy (MA) is a critical property of ferromagnetic material and has been a significant subject of magnetism for a long time [1,2]. In particular, the relations among the MA, the spin-orbit interaction (SOI), and the orbital angular momentum (OAM) have been intensively studied from the aspects of both theory and experiment. In magnetic materials composed of rare-earth elements, spin angular momentum (SAM), S , and the OAM, L , couple strongly due to a large SOI, therefore, the quantity $J = S + L$ is a good quantum number. A large MA appears due to the interaction between the electron charge cloud of the $4f$ orbital and the crystal field. As for the transition-metal (TM) ferromagnets, the OAM is usually quenched at zero; however, a tiny amount of the OAM survives in magnets with low lattice symmetry. Bruno [3] proposed that the uniaxial MA energy (K_u) of a monolayer is proportional to the anisotropy of the OAM $\Delta L = L_x - L_z$, where x and z are the in-plane and out-of-plane directions, respectively, of the monolayer. In this model, the SOI is treated as a second-order perturbation for the tight-binding approximation.

Recently, experimental examinations of the effectiveness of Bruno's model have been performed by using x-ray magnetic circular dichroism (XMCD), which is an atom-specific method used to measure both the SAM and the OAM. For example, Grange *et al.* [4] reported the anisotropy of the OAM obtained by XMCD for Co-Pt thin films and compared them with those calculated by the first principles. Andersson *et al.* [5] studied the relation between OAM and K_u for Au/Co/Au trilayers and pointed out that the OAM anisotropy is not proportional to K_u . Okabayashi *et al.* [6] reported the anisotropy of the OAM using XMCD for Co₂FeAl films on MgO substrates and attributed it to the perpendicular MA caused by an interface effect [7]. Furthermore, Okabayashi *et al.* [8] showed that Bruno's relation holds well for the perpendicular MA at the interface between thin Fe/MgO films prepared under different annealing temperatures. This result

is consistent with the theoretical results of MA energy for transition-metal thin films and Fe/MgO interfaces [9,10]. It is important to note that these theories adopted a nonperturbative treatment of SOI and showed that K_u is proportional to the square of SOI.

In the case of magnetic oxides, MA is strongly dependent on the valency of magnetic cations and local lattice deformation through the SOI [11,12]. It was shown that Co²⁺-doped Fe₃O₄ has a large crystalline MA, which is interpreted in terms of the SOI and t_{2g} -level splitting caused by local lattice symmetry [13,14]. If a tetragonal lattice distortion is introduced to spinel ferrites Fe(Co,Fe)₂O₄ in which Co ions are divalent, a large uniaxial MA can be induced [15–17]. In fact, K_u , which is several tens of Merg/cm³, has been realized by controlling the lattice mismatch between Fe(Co, Fe)₂O₄ films and substrates [18–20]. As $L \approx 1$ of the OAM remains in Co²⁺ ions, it may be interesting to study the relation among K_u , L , and the OAM anisotropy ΔL with a direct measurement of the OAM in transition-metal oxides.

The SAM and OAM are the dominant origins of conventional ferromagnetism through exchange coupling and magnetic anisotropy, respectively. Since the OAM is generally a much smaller quantity than the SAM, it can be difficult to ascertain a relation between K_u and OAM. Fortunately, CoMnO₃ (CMO) is a material that can be used to observe the relation directly for several reasons [21–23]. First, CMO has an ilmenite structure ($R\bar{3}$) in which Co²⁺ and Mn⁴⁺ layers are alternately stacked along the c axis. Second, the SAM of Co²⁺ ($3d^7: S = 3/2$) and Mn⁴⁺ ($3d^3: S = 3/2$) cancel out due to antiferromagnetic coupling. Third, Co²⁺ has an OAM ($L \approx 1$), therefore, the saturation magnetization M_S has a single contribution from the OAM of Co²⁺ ($\langle L \rangle$) such that this compound is termed an “orbital ferrimagnet.” Finally, CMO has a Néel temperature (T_N) of 391 K, and its temperature dependence of M_S , $M_S(T)$ can be measured easily. Because of the large OAM, CMO possesses significantly large in-plane MA (−14 to −16 Merg/cm³) [24,25]. Recently, we have succeeded in fabricating CMO epitaxial thin films on

α -Al₂O₃(0001) [25] by using reactive radio-frequency (rf) magnetron sputtering [26,27]. By using XMCD, we clarified that CMO films on α -Al₂O₃(0001) are, indeed, an orbital ferrimagnet and successfully performed a quantitative comparison between L and magnetization at room temperature.

In this paper, we report the temperature dependence of $K_u(T)$ and $M_S(T)$ of CMO and find a simple relation among $K_u(T)$, $M_S(T)$, and $\langle L \rangle$ that holds for a wide temperature range up to near the transition temperature. Due to the strong in-plane MA of CMO, it takes very high fields to bring M_S parallel to the hard axis, which makes it difficult to perform XMCD experiments. Therefore, in order to discuss the relation between ΔL and K_u , we perform tight-binding calculations for Co-O and Mn-O clusters and investigate the L and ΔE .

This paper is organized as follows. The experiment procedure are explained in Sec. II. Section III is devoted to the experimental results of $M_S(T)$ and $K_u(T)$ as well as calculated results. The final section gives a summary of the works.

II. EXPERIMENT

CMO thin films with thickness of 90 nm were grown on α -Al₂O₃(0001) substrates by reactive rf-magnetron sputtering (ES-250MB: Eiko Engineering Co., Ltd.) [25]. We used a 2-in. alloy target with a Co: Mn = 1:1 composition. The growth conditions of the CMO thin films were as follows: O₂/Ar flow ratios were approximately 0.12, the process temperature was 710 °C, and working pressure was 0.75 Pa. We observed the surface state of the film by the reflection high-energy electron-diffraction technique. The film thicknesses and crystal structure were, respectively, determined by x-ray reflectivity and x-ray diffraction with Cu $K\alpha$ radiation. After sample fabrication, M_S and the K_u were determined by a vibrating sample magnetometer and magnetotorque meter, respectively. Both measurements were performed with a physical property measurement system (Quantum Design).

III. RESULTS AND DISCUSSION

A. Temperature dependence of saturation magnetization

In order to measure the M - H loop, the magnetic field was applied along the in-plane $[11\bar{2}0]$ direction up to 90 kOe. Note that the out-of-plane M - H loop could not be saturated even at 90 kOe, indicating that the film possesses a large negative MA. Figure 1 shows M - H loops of the film at 100, 200, 300, 350, and 400 K. It is known that the epitaxial film of CMO grown on α -Al₂O₃ has a nonmagnetic dead layer that is 21-nm thick [25]. Therefore, we evaluated the M_S by taking the dead layer into account.

In order to investigate $M_S(T)$, we carried out $M(H)$ measurements at various temperatures ranging from 100 to 400 K. $M_S(T)$ was obtained by extrapolation using a linear fit analysis of 21 high-field data points ranging from 70 to 90 kOe. Figure 2 shows $M_S(T)/M_S(0\text{ K})$ of our sample and that of the previous report [21]. The T_N of the film is approximately 385 K, which is close to the previously reported value of T_N for CoMnO₃. Note that the shape of $M_S(T)$ is also similar to Q -type ferrimagnetism but totally different from the other three types of ferrimagnetism, such as the R , P , and N types

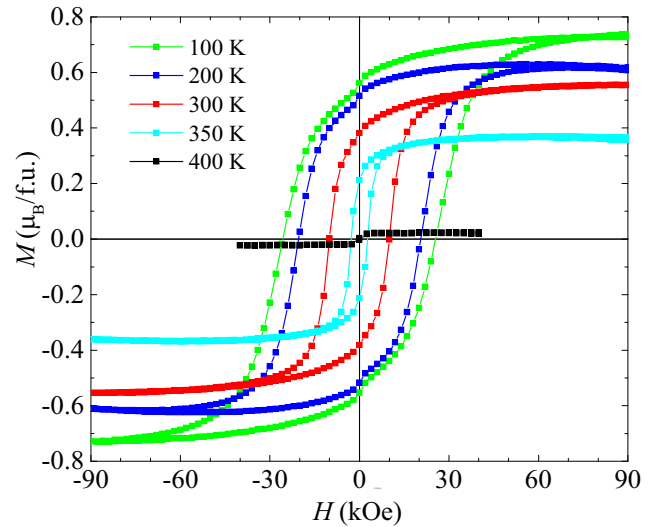


FIG. 1. Temperature dependence of M - H loops of a CMO film. M_S values were determined by the total magnetic moment divided by the intrinsic volume, excluding the dead layer thickness.

[2,28]. However, the magnitudes of the angular momentum of Co²⁺ ($J \approx 5/2$) and Mn⁴⁺ ($J \approx S = 3/2$) are similar, so the observed $M_S(T)$ should be different from Q -type ferrimagnetism.

In order to elucidate the observed results of $M_S(T)$, we adopted the following simple model and used it to calculate the temperature dependence of the OAM $L(T)$. Because the SOI is relatively weak in 3d elements, the SAM and OAM should be treated as weakly dependent quantities. In our system, we need to consider three exchange interactions $J_{\text{Co-Co}}$, $J_{\text{Mn-Mn}}$, and $J_{\text{Co-Mn}}$, between the localized spins of Co and Mn ions. In the molecular field approximation (MFA), we assume, for simplicity, that the thermal average of the SAM $\langle S \rangle$ of Co and Mn are the same except for their sign. Then, the exchange field acting on the Co and Mn spins may be given as $(nJ_{\text{Co-Co}} - n'J_{\text{Co-Mn}}) \langle S \rangle_i$ and $-(nJ_{\text{Mn-Mn}} -$

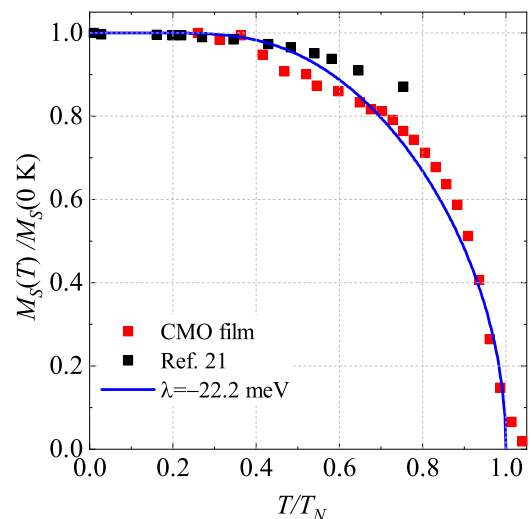


FIG. 2. The temperature dependence of the film from Ref. [21] and Eq. (2).

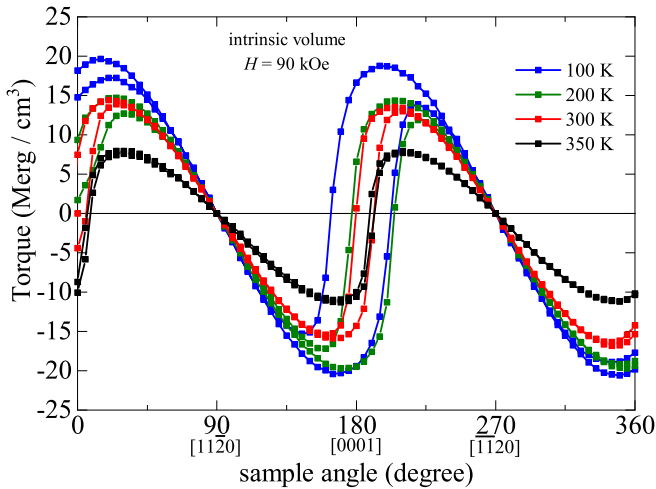


FIG. 3. Temperature dependence of the magnetotorque curve of the film.

$n'J_{\text{Co-Mn}} \langle S \rangle_i$, respectively, where n and n' are the number of nearest-neighbor sites of Co and Mn around Co ions, respectively. The definition of n and n' around Mn ions is the same because of the lattice symmetry.

By the relationship $(nJ_{\text{Co-Co}} - n'J_{\text{Co-Mn}}) = \tilde{n}\tilde{J}$, the effective MFA Hamiltonian for the Co sublattice (i site) in zero field, $H = 0$ is given as

$$\mathcal{H}_{\text{Co},i} = (-\tilde{n}\tilde{J}S_{\text{Co},i} + \lambda L_i) \langle S \rangle, \quad (1)$$

where λ is the magnitude of the SOI. We approximate $\tilde{n}\tilde{J} \langle S \rangle - \lambda \langle L \rangle \approx \tilde{n}\tilde{J} \langle S \rangle$ because the exchange coupling, in general, is larger than the SOI. The calculated result of the OAM is given as

$$\langle L \rangle = \tanh \left(\frac{-\lambda \langle S \rangle}{k_B T} \right), \quad (2)$$

where $\langle S \rangle$ is obtained by the MFA for $S = 3/2$. The magnitude of \tilde{J} is fixed to give T_N . Moreover, we treated λ as a parameter in Eq. (2) and performed curve fitting to $M_S(T)$ because $\langle L \rangle$ is the total magnetization. The fitted result gives $\lambda = -22.2 \pm 0.5$ meV, which is close to the previously reported value of $\lambda = -20$ meV for Co^{2+} in Fe_3O_4 [13].

B. Temperature dependence of K_u

The temperature dependence of the magnetic torque curves at 100, 200, 300, and 350 K of the film is shown in Fig. 3. We note that a rotational hysteresis opens up near the transition temperature, meaning that the magnetic anisotropy field ($H_A = 2|K_u|/M_S$) is much larger than our applied field of 90 kOe. In the following, K_u is determined from the peak-to-peak value of the magnetotorque curve.

The plot of $K_u(T)$ versus $M_S(T)$ for $T = 110$ to 390 K is shown in Fig. 4. It can be seen that all the data lie on a single straight line. Because $K_u(T)$ is simply proportional to $M_S(T)$ over a wide temperature range up to T_N , H_A is temperature independent. Because M_S corresponds to the OAM, this means that K_u is proportional to $\langle L \rangle$ as well. Note that H_A estimated from the slope in Fig. 4 is 272 ± 13 kOe.

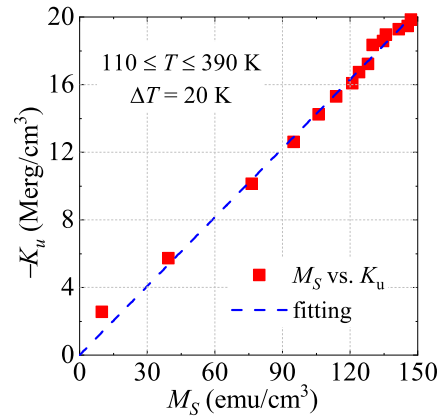


FIG. 4. The temperature dependence of $M_S(= \langle L \rangle)$ versus the K_u plot.

In most magnetic oxides, the origin of MA is attributed to (i) dipole-dipole interaction, and/or (ii) the SOI of magnetic ions, such as the single-ion anisotropy model [29]. MA originated from dipole-dipole interaction gives $2\pi M_S^2$. In the case of the single-ion anisotropy model, MA originates from spin correlation through the SOI and crystal field, which gives $K_u(T) \propto M_S(T)^{l(l+1)/2}$ [30–33], where l is an exponent that is dependent on crystal symmetry and the degree of correlation between the directions of adjacent spins. In this model, the SOI is treated as a second-order perturbation. In the case of uniaxial MA systems, $l(l+1)/2$ is predicted to be 3. Although Fig. 4 implies $l = 1$ for our results, this exponent cannot be explained by either of the above two models.

C. Electron theory

In our experiments, the large value of H_A prevents us from performing XMCD measurements to find M_S with out-of-plane angles. Therefore, to reveal a relation between K_u and ΔL and to understand the experimental results of the K_u - M_S relation, we performed numerical calculations of L_x , L_z , and the d -orbit energy level for clusters with a single Mn^{4+} or Co^{2+} ion surrounded by six (octahedral cluster) O^{2-} ions. The electronic structure of the cluster was calculated by using a tight-binding model for $3d$ and $2p$ orbitals of TM ions and oxygen ions, respectively, and by including the SOI $\lambda_c \ell \cdot s$, where ℓ and s are the orbital-angular operator and spin operator, respectively, for $3d$ -electrons on Co or Mn ions [34]. It is assumed that the $3d$ states of Co and Mn ions are fully spin polarized, and the ions have local moments. The clusters are simplified models, but they satisfy the local symmetry. Parameters of intersite p - d hopping between $3d$ orbitals on a TM ion and $2p$ orbitals on oxygen ions are determined from Harrison's textbook [35,36]. The electron configuration for Mn^{4+} is $3d^3$, Co^{2+} is $3d^7$, and O^{2-} is $2p^6$.

The ground-state energy is calculated by diagonalizing the Hamiltonian matrix as a function of magnetization direction. It is noted that the mixing of p and d orbitals reproduces the correct symmetry dependence of energy levels as in the crystal-field potentials. The Wyckoff positions of CMO are adopted from the previous report in Ref. [22].

Figure 5 shows the calculated results of the t_{2g} energy levels as a function of SOI, in other words, λ_c . The calculation

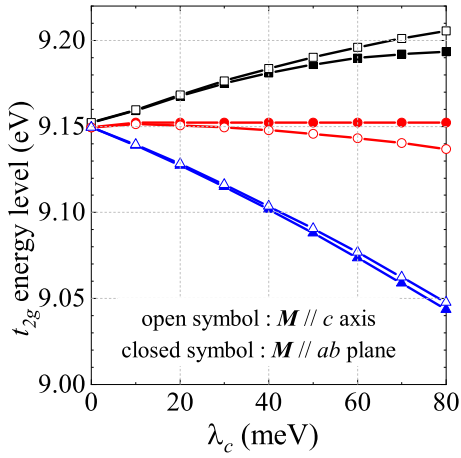


FIG. 5. The relation between the t_{2g} orbital and λ_c . Lines of the same color represent the same orbit, open symbols denote the $\mathbf{M} \parallel c$ axis, and closed symbols denote the $\mathbf{M} \parallel ab$ plane.

was performed under the following two conditions: (i) the magnetic moment (\mathbf{M}) points to the c -axis direction, (ii) \mathbf{M} points to the ab plane. If $\lambda_c = 0$ meV, there remains double degeneracy in the t_{2g} state. Because the electron configuration of the Co^{2+} ion is $3d^7$, the lower two energy levels of the down-spin t_{2g} states are occupied. Figure 5 shows that with increasing λ_c , the shift of the energy level (shown by circles) due to the change in the \mathbf{M} direction is the largest, and therefore, MA energy becomes high. On the other hand, the electron configuration of the Mn^{4+} ion is $3d^3$, and the up-spin t_{2g} levels are fully occupied. As a result, the MA energy is low.

Figures 6(a) and 6(b) show the calculated results of L_x , L_z , and $\Delta L \equiv L_x - L_z$ as a function of λ_c for Co and Mn ions. We

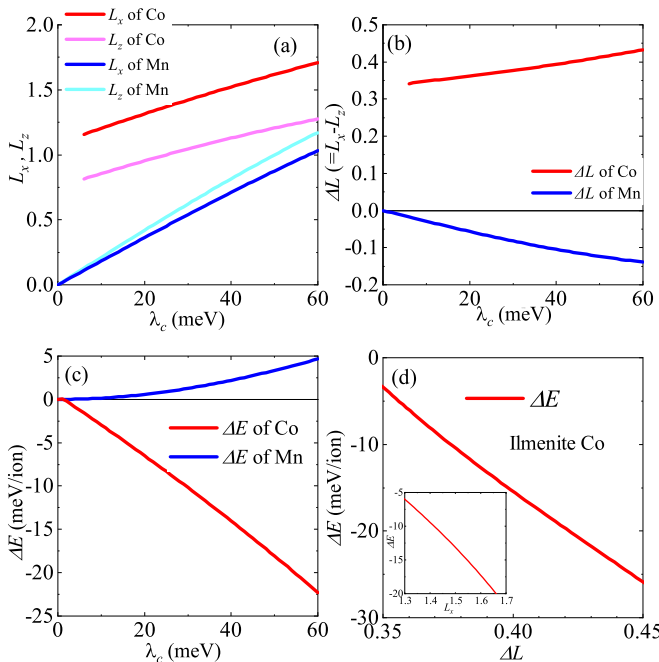


FIG. 6. The relations between λ_c versus (a) L_x , L_z , and (b) ΔL of both cations. (c) The relation between λ_c versus ΔE . (d) The relation between ΔL and ΔE of Co^{2+} , and the inset shows L_x versus ΔE .

find ΔL depends almost linearly on λ_c . Figure 6(c) shows the calculated results of $\Delta E \equiv E_x - E_z$, which is K_u , for Co and Mn. We find Co^{2+} has a negative MA whereas Mn^{4+} has a positive MA. Because the magnitude of K_u is much larger for Co^{2+} than Mn^{4+} , CMO has a negative K_u . This means that the easy axis of CMO lies on the ab plane, which is consistent with the magnetotorque measurement. Moreover, assuming $|\lambda_c| = 20$ meV, K_u is approximately -38 Merg/cm³. This is almost twice the measured value of -20.1 ± 1.0 Merg/cm³ at 100 K. Since rotational hysteresis is observed in the torque measurement, the intrinsic K_u of CMO must be larger than -20.1 ± 1.0 Merg/cm³. We, thus, conclude that the calculation results are semiquantitatively consistent with experimental results.

Because we found that the dominant component contributing to MA is that of Co^{2+} , in the following discussion, we consider only Co^{2+} . Figure 6(d) shows ΔE as a function of ΔL for Co^{2+} . ΔL for Co has a near-linear dependence on λ_c as shown in Fig. 6(b), and ΔE linearly changes with λ_c for Co as shown in Fig. 6(c). Therefore, ΔE depends linearly on ΔL for Co.

The result that K_u is proportional to ΔL for Co^{2+} is attributed to the following facts: (i) The down spins of the t_{2g} states are partially occupied by electrons, (ii) the energy gap between the t_{2g} and the e_g levels is much larger than the SOI, and (iii) the energy gaps between the t_{2g} levels are the same order of magnitude with that of SOI. Actually, we found that K_u is proportional to $(\Delta L)^2$ when the SOI is much smaller than the energy splitting between the t_{2g} states caused by the crystal-field potential (p - d mixing in the present case is not shown). We, thus, conclude the dependence of K_u on ΔL is governed by the relative magnitude of the SOI and energy-level splitting of the $3d$ states. Note that, in the electron theory, we calculate the OAM of Co^{2+} at 0 K, however, the magnetization of CMO is the thermal average value of the OAM.

Because the $K_u (= \Delta E)$ of CMO is dominated by that of Co^{2+} and $\langle L \rangle$ originates from the OAM of Co^{2+} , the K_u of CMO is proportional to $\langle L \rangle$ of CMO. Furthermore, as shown in Fig. 6(c), K_u is proportional to ΔL . This result coincides with Bruno's model, which treated SOI as a second-order perturbation. However, a careful interpretation is necessary. Because L_{Co} is comparable to S_{Co} in CMO, L_{Co} cannot be treated within the framework of second-order perturbation.

IV. CONCLUSION

In this paper, $M_S(T)$ and $K_u(T)$ of *orbital ferrimagnet* CoMnO_3 films were carefully investigated over a wide temperature range. We succeeded in explaining the observed $M_S(T)$ through the temperature dependence of the OAM $L(T)$, calculated within the framework of the MFA.

We also found that $K_u(T)$ was linearly proportional to $M_S(T)$, meaning that $K_u(T)$ is simply proportional to $L(T)$. We conclude that the relation $K_u \propto \langle L \rangle$ holds even for large OAMs. Numerical calculations of the OAM and the d -orbital energy level for clusters suggest that K_u is proportional to ΔL . Further experimental verification is necessary for a unified understanding of the behavior of K_u . We note that the M_S of CMO is expected to be highly anisotropic because of the distinct difference between L_x and L_z for Co^{2+} as shown in

Fig. 6(a). A high-field experiment with the bulk single-crystal CMO can make the difference of L_x and L_z clear.

ACKNOWLEDGMENTS

This work was performed under the approval of the Photon Factory Program Advisory Committee (Proposals No.

2017G602 and No. 2016S2-005). H.K. acknowledges the Kato Foundation for Promotional Science. This project is partly supported by Japan Science and Technology Agency (JST) under Collaborative Research Based on Industrial Demand “High Performance Magnets: Towards Innovative Development of Next Generation magnets” (Grant No. JP-MJSK1415).

-
- [1] R. M. Bozorth, *Ferromagnetism* (Wiley-IEEE Press, Hoboken, NJ, 1978).
- [2] S. Chikazumi and C. D. Graham, *Physics of Ferromagnetism* (Oxford University Press, New York, 1997).
- [3] P. Bruno, *Phys. Rev. B* **39**, 865 (1989).
- [4] W. Grange, I. Galanakis, M. Alouani, M. Maret, J.-P. Kappler, and A. Rogalev, *Phys. Rev. B* **62**, 1157 (2000).
- [5] C. Andersson, B. Sanyal, O. Eriksson, L. Nordström, O. Karis, D. Arvanitis, T. Konishi, E. Holub-Krappe, and J. H. Dunn, *Phys. Rev. Lett.* **99**, 177207 (2007).
- [6] J. Okabayashi, H. Sukegawa, Z. Wen, K. Inomata, and S. Mitani, *Appl. Phys. Lett.* **103**, 102402 (2013).
- [7] Z. Wen, H. Sukegawa, S. Mitani, and K. Inomata, *Appl. Phys. Lett.* **98**, 242507 (2011).
- [8] J. Okabayashi, J. W. Koo, H. Sukegawa, S. Mitani, Y. Takagi, and T. Yokoyama, *Appl. Phys. Lett.* **105**, 122408 (2014).
- [9] A. Lessard, T. H. Moos, and W. Hübner, *Phys. Rev. B* **56**, 2594 (1997).
- [10] H. X. Yang, M. Chshiev, B. Dieny, J. H. Lee, A. Manchon, and K. H. Shin, *Phys. Rev. B* **84**, 054401 (2011).
- [11] R. M. Bozorth, E. F. Tilden, and A. J. Williams, *Phys. Rev.* **99**, 1788 (1955).
- [12] J. Smit and H. P. J. Wijn, *Ferrite* (Philips Technical Library, Eindhoven, 1959).
- [13] J. C. Slonczewski, *Phys. Rev.* **110**, 1341 (1958).
- [14] M. Tachiki, *Prog. Theor. Phys.* **23**, 1055 (1960).
- [15] Y. Suzuki, G. Hu, R. van Dover, and R. Cava, *J. Magn. Magn. Mater.* **191**, 1 (1999).
- [16] A. Lisfi, C. M. Williams, L. T. Nguyen, J. C. Lodder, A. Coleman, H. Corcoran, A. Johnson, P. Chang, A. Kumar, and W. Morgan, *Phys. Rev. B* **76**, 054405 (2007).
- [17] J. Inoue, H. Itoh, M. A. Tanaka, K. Mibu, T. Niizeki, H. Yanagihara, and E. Kita, *IEEE Trans. Magn.* **49**, 3269 (2013).
- [18] T. Niizeki, Y. Utsumi, R. Aoyama, H. Yanagihara, J. Inoue, Y. Yamasaki, H. Nakao, K. Koike, and E. Kita, *Appl. Phys. Lett.* **103**, 162407 (2013).
- [19] H. Onoda, H. Sukegawa, E. Kita, and H. Yanagihara, *IEEE Trans. Magn.* **54**, 1 (2018).
- [20] T. Tainosho, J. Inoue, S. Sharmin, M. Takeguchi, E. Kita, and H. Yanagihara, *Appl. Phys. Lett.* **114**, 092408 (2019).
- [21] R. M. Bozorth and D. E. Walsh, *J. Phys. Chem. Solids* **5**, 299 (1958).
- [22] W. H. Cloud, *Phys. Rev.* **111**, 1046 (1958).
- [23] T. J. Swoboda, R. C. Toole, and J. D. Vaughan, *J. Phys. Chem. Solids* **5**, 293 (1958).
- [24] W. H. Cloud and J. P. Jesson, *J. Appl. Phys.* **37**, 1398 (1966).
- [25] H. Koizumi, S. Sharmin, K. Amemiya, M. Suzuki-Sakamaki, J.-i. Inoue, and H. Yanagihara, *Phys. Rev. Mater.* **3**, 024404 (2019).
- [26] H. Yanagihara, M. Myoka, D. Isaka, T. Niizeki, K. Mibu, and E. Kita, *J. Phys. D: Appl. Phys.* **46**, 175004 (2013).
- [27] T. Ojima, T. Tainosho, S. Sharmin, and H. Yanagihara, *AIP Adv.* **8**, 045106 (2018).
- [28] M. L. Néel, *Ann. Phys.* **12**, 137 (1948).
- [29] J. M. D. Coey, *Magnetism and Magnetic Materials* (Cambridge University Press, New York, 2010).
- [30] C. Zener, *Phys. Rev.* **96**, 1335 (1954).
- [31] F. Keffer, *Phys. Rev.* **100**, 1692 (1955).
- [32] J. Van Vleck, *J. Phys. Radium* **20**, 124 (1959).
- [33] H. Callen and E. Callen, *J. Phys. Chem. Solids* **27**, 1271 (1966).
- [34] J. Inoue, H. Nakamura, and H. Yanagihara, *Hard and Soft Magnetic Materials* **3**, 12 (2019).
- [35] W. A. Harrison, *Electronic Structure and the Properties of Solids*, Dover Books on Physics (Dover, New York, 1989).
- [36] J. Inoue, *J. Phys. D: Appl. Phys.* **48**, 445005 (2015).